Journal for ImmunoTherapy of Cancer

Distinct exhaustion features of T lymphocytes shape the tumor-immune microenvironment with therapeutic implication in patients with non-small-cell lung cancer

Chang Gon Kim,[1] Gamin Kim,[1] Kyung Hwan Kim,[2] Seyeon Park,[3] Sunhye Shin,[1] Dahee Yeo,[1] Hyo Sup Shim,[4] Hong In Yoon,[2] Seong Yong Park ,[5] Sang-Jun Ha ,[3] Hye Ryun Kim [1]

To cite: Kim CG, Kim G, Kim KH, *et al*. Distinct exhaustion features of T lymphocytes shape the tumor-immune microenvironment with therapeutic implication in patients with non-small-cell lung cancer. *Journal for ImmunoTherapy of Cancer* 2021;**9**:e002780. doi:10.1136/jitc-2021-002780

► Additional supplemental material is published online only. To view, please visit the journal online (http://dx.doi.org/10.1136/jitc-2021-002780).

CGK and GK are joint first authors.

Accepted 07 October 2021

For numbered affiliations see end of article.

Correspondence to
Professor Hye Ryun Kim; nobelg@yuhs.ac

Professor Sang-Jun Ha; sjha@yonsei.ac.kr

Professor Seong Yong Park; syparkcs@yuhs.ac

ABSTRACT

Background Reinvigoration of T-cell exhaustion with antibodies has shown promising efficacy in patients with non-small-cell lung cancer (NSCLC). However, the characteristics of T-cell exhaustion with regard to tumor-infiltrating lymphocytes (TILs) are poorly elucidated in NSCLC. Here, we investigated the exhaustion status of TILs in NSCLC patients at the intraindividual and interindividual levels.

Methods We obtained paired peripheral blood, normal adjacent tissues, peritumoral tissues, and tumor tissues from 96 NSCLC patients. Features of T-cell exhaustion were analyzed by flow cytometry. T cells were categorized according to their programmed cell death-1 (PD-1) expression (PD-1^{high}, PD-1^{int}, and PD-1^{neg} cells). Patients were classified based on the presence or absence of discrete PD-1^{high} CD8^{+} TILs. Production of effector cytokines by CD8^{+} TILs was measured after T-cell stimulation with or without antibodies against immune checkpoint receptors.

Results Progressive T-cell exhaustion with marked expression of exhaustion-related markers and diminished production of effector cytokines was observed in PD-1^{high} CD8^{+} TILs compared with PD-1^{int} and PD-1^{neg} CD8^{+} TILs. Patients with distinct PD-1^{high} CD8^{+} TILs (PD-1^{high} expressers) exhibited characteristics associated with a favorable anti-PD-1 response compared with those without these lymphocytes (non-PD-1^{high} expressers). Combined inhibition of dual immune checkpoint receptors further restored effector cytokine production by CD8^{+} TILs following T-cell stimulation. PD-1^{high} CD8^{+} T lymphocyte populations in the peripheral blood and tumors were significantly correlated.

Conclusions T-cell exhaustion was differentially regulated among individual patients and was prominent in a subgroup of NSCLC patients who may benefit from PD-1 blockade or combined blockade of other immune checkpoint receptors.

BACKGROUND

T-cell exhaustion is a distinct type of T-cell dysfunction that develops during cancers and chronic infections.[1] Exhausted T cells are characterized by progressive loss of effector functions, high and sustained expression of immune checkpoint inhibitory receptors, poor memory recall, metabolic dysregulation, and diminished homeostatic self-renewal.[2] Of note, T-cell exhaustion is accompanied by transcriptional and epigenetic reprogramming during chronic T-cell receptor stimulation without antigenic clearance.[3–7] Nowadays, targeting immune checkpoint receptors, including programmed cell death-1 (PD-1) and cytotoxic T-lymphocyte-associated protein-4 (CTLA-4), has been developed for reinvigorating exhausted T cells.[8 9] In non-small-cell lung cancer (NSCLC), anti-PD-1 antibodies such as pembrolizumab and nivolumab used as monotherapies or as combination therapy with chemotherapy or other immune checkpoint inhibitors have substantially improved survival outcomes.[10–16] However, it is noteworthy that only a minor proportion of patients derive therapeutic benefits from immune checkpoint inhibitors.[17 18] Thus, further improvements in immunotherapeutic strategies based on an in-depth understanding of T-cell exhaustion are required to improve patient responses and outcomes.

Currently, expression of programmed death ligand-1 (PD-L1),[19 20] spatial and temporal distribution of tumor-infiltrating lymphocytes (TILs),[21] tumor mutation burden,[22] gene expression profiles,[23] and human leucocyte antigen heterogeneity[24] have been suggested as biomarkers to predict the response to PD-1 blockade.[25] In NSCLC, two key oncogenic alterations, epidermal growth factor receptor (EGFR) mutations and anaplastic lymphoma

kinase (*ALK*) rearrangements, have been proposed to predict low response rates to anti-PD-1 treatment.[20 26] However, only a few studies have evaluated the exhaustion of TILs, a direct target population of immune checkpoint blockade in the tumor microenvironment (TME), in patients with NSCLC. Investigation of T-cell exhaustion in tumor tissues from patients can provide mechanistic insights into the prediction of treatment response and resistance, as well as a basis for enhancing the therapeutic efficacy of combinatorial strategies.

In this study, we characterized the exhaustion of TILs in NSCLC by focusing on the expression of immune checkpoint receptors using freshly collected surgically resected tumor tissues. Further, we performed a correlation analysis of T-cell exhaustion with clinicopathological variables such as smoking status, histological subtype, alterations of *EGFR* or *ALK*, PD-L1 expression, and survival outcomes. Thus, we conceived an ex vivo model system to display anti-PD-1 responses in vivo and suggest a strategy for enhancing the therapeutic benefits of PD-1 blockade. Finally, we propose a peripheral blood-derived biomarker to predict T-cell exhaustion status in the TME.

MATERIALS AND METHODS

Specimen collection and preparation

Tissue specimens were collected at Yonsei Cancer Center (Seoul, Republic of Korea) from 96 patients with NSCLC who agreed to participate in the study from August 2017 to June 2021. Normal adjacent tissues (at least 5 cm away from gross tumor tissues) and peritumoral tissues (within 1 cm of gross tumor tissues) were obtained if required. Fresh tissue was cut into 1 mm^3 pieces and digested with 1 mg/mL collagenase type IV (Worthington Biochemical, Lakewood, New Jersey, USA) and 0.01 mg/mL DNase I (Sigma-Aldrich, St. Louis, Missouri, USA) at 37°C for 20 min. The dissociated tissues were filtered through a 40 µm cell strainer (Corning, Corning, New York, USA) and washed with Roswell Park Memorial Institute-1640 medium (Corning) containing 10% fetal bovine serum (Biowest, FRA) and centrifuged. Tissue-infiltrating lymphocytes were enriched using a Percoll gradient (Sigma-Aldrich) followed by the staining of single-cell suspensions with the indicated fluorescent-conjugated antibodies.

Flow cytometry

Cells were stained with antibodies against cell-surface molecules for 20 min at 4°C. The LIVE/DEAD Fixable Red Dead Cell Stain Kit (Thermo Fisher Scientific, Waltham, Massachusetts, USA) was used to identify live cells. For intracellular staining, cells were fixed and permeabilized with the Foxp3 fixation/permeabilization solution (ThermoFisher Scientific) for 20 min at 4°C, and stained with antibodies against intracellular molecules for 20 min at 4°C. The stained cells were analyzed using FACS CytoFLEX (Beckman Coulter, Brea, California, USA) and the data were analyzed using FlowJo software V.10 (Treestar, San Carlos, California, USA). The antibodies used are listed in online supplemental table 1 and the gating strategies for flow cytometry are shown in online supplemental figure 1. Expression of PD-1 on $CD8^+$ T lymphocytes from peripheral blood was used to gate for $PD\text{-}1^{neg}$, $PD\text{-}1^{int}$, and $PD\text{-}1^{high}$ populations.

Intracellular cytokine secretion assay

For the intracellular cytokine analysis of TILs, cells from dissociated tumors in the density range of 1×10^5 to 1×10^6 cells were cultured in a 96-well U-bottom plate containing 10 µg/mL of pembrolizumab (Selleckchem, Houston, Texas, USA), 10 µg/mL of ipilimumab (Selleckchem), soluble 50 ng/mL of anti-CD3 (BD Biosciences, San Jose, California, USA), and 50 ng/mL of anti-CD28 (BD Biosciences) for 24 hours at 37°C, followed by the addition of brefeldin A (BD Biosciences) and monensin (BD Biosciences) per the manufacturer's protocol. To measure interferon (IFN)-γ and tumor necrosis factor (TNF) secretion levels by $CD8^+$ TILs according to PD-1 expression on anti-CD3 and anti-CD28 stimulation, the pre-incubation step without brefeldin A and monensin for 24 hours was omitted. After 12 hours, the cells were harvested and stained. Intracellular cytokines were stained after surface staining, fixation, and permeabilization with Foxp3 fixation/permeabilization solution (Thermo Fisher Scientific).

Three-dimensional imaging of live cells

Three samples each from $PD\text{-}1^{high}$ and non-$PD\text{-}1^{high}$ expressers were used for live cell imaging analysis using t-stochastic neighbor embedding (t-SNE), a tool for visualizing high-dimensional data. Each sample was downsampled to 20,000 randomly selected $CD3^+$ live and singlet-gated cells. A total of 60,000 cells were merged. Then, 53,574 cells among 120,000 total cells were gated for $CD8^+$ and visualized using t-SNE for analysis using FlowJo software V.10.6.2 (Treestar) with 3,000 iterations and a perplexity parameter of 100.

PD-L1 expression in tumor tissues

PD-L1 expression in the archived specimens was determined by immunohistochemical analysis using anti-PD-L1 antibodies (clone SP263). The tumor proportion score was determined for the positivity of PD-L1 expression on tumor cells as described previously.[27] PD-L1 expression in freshly collected surgically resected tumor tissues was determined by flow cytometry.

Statistical analysis

Statistical significance was assessed using two-tailed Student's t-test, χ^2 test, or one-way analysis of variance with Tukey's correction, as appropriate, with the Prism .7.0 software (GraphPad). Values of $p\leq0.05$ (*), ≤0.01 (**), ≤0.001 (***), and ≤0.0001 (****) were considered significant.

RESULTS

CD8+ TILs from NSCLC patients were subdivided into three distinct subpopulations based on PD-1 expression

First, we examined PD-1 expression on CD8+ T lymphocytes from the peripheral blood, normal adjacent tissues, peritumoral tissues, and tumor tissues of patients with NSCLC (figure 1A). The frequency of PD-1+ cells among CD8+ T lymphocytes was the highest in CD8+ TILs, followed by CD8+ T lymphocytes from peritumoral tissues, normal adjacent tissues, and peripheral blood (figure 1B). We then subdivided CD8+ T lymphocytes into three distinct populations based on PD-1 expression: PD-1neg, PD-1int, and PD-1high (figure 1A). PD-1neg CD8+ T lymphocytes constituted the major population of CD8+ T lymphocytes from peripheral blood samples, whereas PD-1high CD8+ T lymphocytes were relatively enriched in CD8+ TILs (figure 1B–E). Notably, PD-1+ cells in CD8+ T lymphocytes from peripheral blood samples were mostly distributed in PD-1int populations (figure 1C). Importantly, the frequency of PD-1high CD8+ T cells was positively correlated among the normal adjacent tissues, peritumoral tissues, and tumor tissues (online supplemental figure 2), indirectly supporting field cancerization.[28]

To further understand the characteristics of CD8+ TILs distinguished by differential PD-1 expression, we investigated the expression pattern of other immune checkpoint receptors such as T cell immunoglobulin and mucin domain-containing protein 3 (TIM-3), T cell immunoreceptor with Ig and ITIM domains (TIGIT), and cytotoxic T-lymphocyte-associated protein-4 (CTLA-4) in PD-1high, PD-1int, and PD-1neg CD8+ TILs (figure 1F–H and K–M). Notably, the expression of these immune checkpoint inhibitory receptors was predominantly observed in the PD-1high population, suggesting more progressed T-cell exhaustion features in this population. Expression of the costimulatory molecule inducible T-cell costimulator (ICOS) and the proliferation marker Ki-67 was also higher in the PD-1high population than in the PD-1int and/or PD-1neg populations (figure 1I,J and N,O), suggesting the indispensable relationship between T-cell activation and exhaustion.[29] Of note, tissue-resident memory CD8+ T lymphocytes co-expressing CD39 and CD103 were significantly enriched in PD-1high populations (online supplemental figure 3), consistent with previous reports.[30 31] The same results were observed when we examined tumor-infiltrating FoxP3− non-Treg and FoxP3+ Treg CD4+ T lymphocytes for the percentages of TIM-3+, TIGIT+, CTLA-4+, ICOS+, and Ki-67+ cells based on their PD-1 expression (online supplemental figures 4 and 5). In addition, there was a strong correlation between the frequency of PD-1high or PD-1+ cells among tumor-infiltrating CD8+, FoxP3− non-Treg, and FoxP3+ Treg CD4+ T lymphocytes (online supplemental figure 6), revealing the shared machinery of PD-1 induction between different T cell populations.[32] Intracellular cytokine staining showed that the population producing effector cytokines was smaller in PD-1high CD8+ T cells than in PD-1int and PD-1neg cells on stimulation with anti-CD3 and anti-CD28 (figure 1P–S). Taken together, these results indicate that the T-cell exhaustion process is largely limited to the TME, and that PD-1high CD8+ TILs present features of more progressed T-cell exhaustion than PD-1int and PD-1neg T lymphocytes, as indicated by the prominent expression of exhaustion-related markers and diminished effector cytokine production, consistent with previous literature.[33 34]

Patients with NSCLC can be classified into two subgroups based on the presence of distinct PD-1high CD8+ TILs

Based on the presence or absence of distinct PD-1high subpopulations in CD8+ TILs, we identified two distinct patient subgroups (figure 2A), namely PD-1high expressers (presence of distinct PD-1high CD8+ TILs) and non-PD-1high expressers (absence of distinct PD-1high CD8+ TILs), via flow cytometric analysis. Consequently, 25 PD-1high expressers (26.0%) and 71 non-PD-1high expressers (74.0%) comprised our cohort (figure 2B). The frequency of PD-1+ cells among CD8+ TILs was higher in PD-1high expressers than in non-PD-1high expressers (figure 2C). Furthermore, the frequency of PD-1+TIM-3+, PD-1+TIGIT+, PD-1+CTLA-4+, and PD-1+ICOS+ cells among CD8+ TILs was significantly higher in PD-1high expressers than in non-PD-1high expressers (figure 2D–G). Similar results were observed in tumor-infiltrating FoxP3− non-Treg and FoxP3+ Treg CD4+ T lymphocytes (figure 2H–Q), further confirming the close relationship between the exhaustion process of different T-cell subsets in the TME. In terms of effector cytokine production, the frequency of IFN-γ+ and/or TNF+ cells was lower in PD-1high expressers than in non- PD-1high expressers (figure 2R–U). Analysis with the t-SNE algorithm showed that the expression of immune checkpoint molecules, including PD-1, TIM-3, TIGIT, CTLA-4, and ICOS, was evidently higher in CD8+ TILs from PD-1high expressers than in those from non-PD-1high expressers (online supplemental figure 7). In line with this observation, the levels of various immune checkpoint inhibitory receptors were positively correlated with each other in bulk tumor tissue samples from The Cancer Genome Atlas NSCLC cohort (online supplemental figure 8), supporting the justification of the combined blockade of immune checkpoint inhibitory receptors in PD-1high expressers.

Clinicopathological characteristics and survival outcomes of PD-1high expressers and non-PD-1high expressers

PD-1high expressers and non-PD-1high expressers did not significantly differ with regard to age and stage. However, PD-1high expressers were more likely to be males with a smoking history and a squamous histology, and had *EGFR* and *ALK* wild-type tumors (table 1, figure 3A–D). Based on the analysis revealing that EpCAM+CD45- cells were major PD-L1 carriers in NSCLC (online supplemental figure 9), we further explored PD-L1 expression on tumor cells via immunohistochemistry. PD-L1 expression on tumor cells was significantly higher in PD-1high expressers than in non-PD-1high expressers both in terms of positivity (cut-off

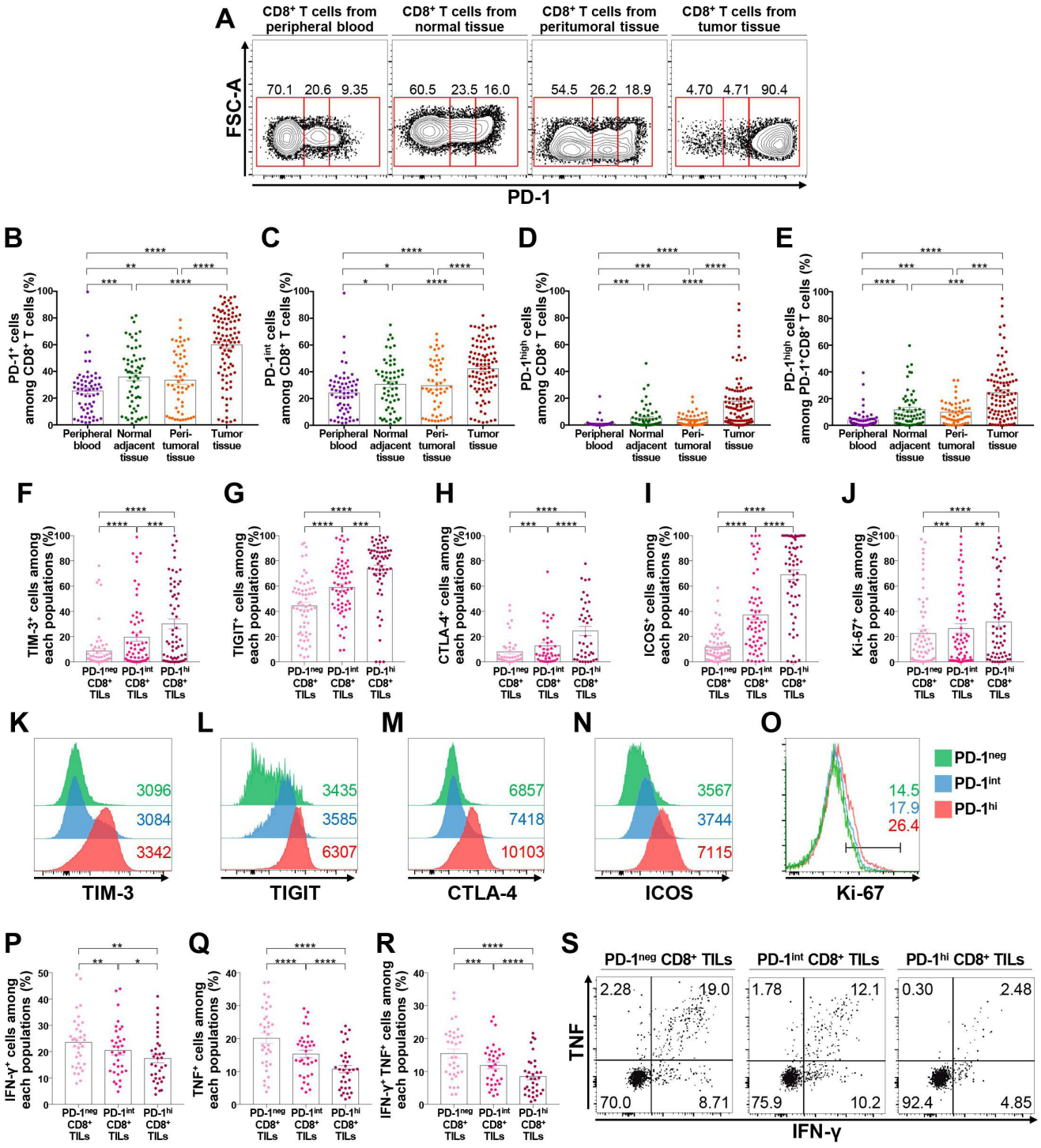

Figure 1 PD-1^{high} CD8$^+$ T lymphocytes are enriched in the tumor-immune microenvironment and highly express exhaustion-related and activation-related molecules. (A–E) Expression of PD-1 in CD8$^+$ T lymphocytes from the peripheral blood, normal adjacent tissue, peritumoral tissue, and tumor tissue from NSCLC patients. Representative flow cytometry plots (A); frequencies of PD-1$^+$ (B), PD-1^{int} (C), and PD-1^{high} (D) cells among CD8$^+$ T lymphocytes; and frequency of PD-1^{high} cells among PD-1$^+$CD8$^+$ T lymphocytes (E). (F–O) Expression of exhaustion-related and activation-related molecules on CD8$^+$ TILs according to PD-1 expression. Representative histogram and the frequency of TIM-3$^+$ (F, K), TIGIT$^+$ (G, L), CTLA-4$^+$ (H, M), ICOS$^+$ (I, N), and Ki-67$^+$ (J, O) cells among CD8$^+$ TILs. (P–S) Production of IFN-γ (P), TNF (Q), and both IFN-γ and TNF (R) of CD8$^+$ TILs on stimulation with anti-CD3 and anti-CD28, and a representative flow cytometry plot (S). *p<0.05; **p<0.01; ***p<0.001; ****p<0.0001. CTLA-4, cytotoxic T-lymphocyte-associated protein-4; FSC-A, forward scatter area; ICOS, inducible T-cell costimulator; IFN-γ, interferon-γ; NSCLC, non-small-cell lung cancer; PD-1, programmed cell death-1; TIGIT, T cell immunoreceptor with Ig and ITIM domains; TILs, tumor-infiltrating lymphocytes; TIM-3, T cell immunoglobulin and mucin domain-containing protein 3; TNF, tumor necrosis factor.

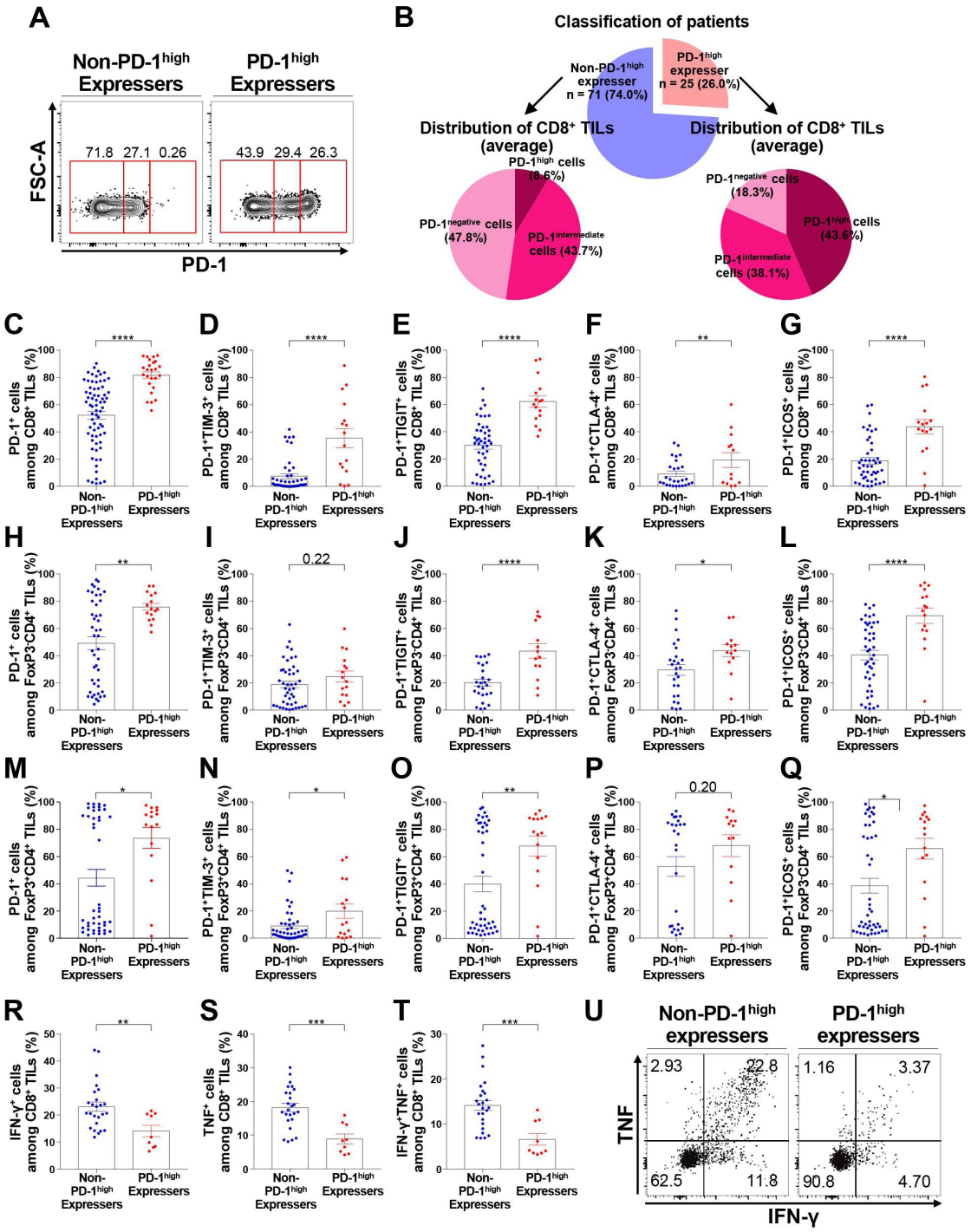

Figure 2 Distinct subgroups of NSCLC patients according to the presence of discrete PD-1^{high} CD8$^+$ TILs. (A) Representative flow cytometry plots showing the two subgroups of NSCLC patients, namely PD-1^{high} expressers and non-PD-1^{high} expressers. (B) Classification of patients and average distribution of PD-1 expression in CD8$^+$ TILs in each subgroup. (C–G) Frequencies of PD-1$^+$ (C), PD-1$^+$TIM-3$^+$ (D), PD-1$^+$TIGIT$^+$ (E), PD-1$^+$CTLA-4$^+$ (F), and PD-1$^+$ICOS$^+$ (G) cells among CD8$^+$ TILs in non-PD-1^{high} expressers and PD-1^{high} expressers. (H–L) Frequencies of PD-1$^+$ (H), PD-1$^+$TIM-3$^+$ (I), PD-1$^+$TIGIT$^+$ (J), PD-1$^+$CTLA-4$^+$ (K), and PD-1$^+$ICOS$^+$ (L) cells among tumor-infiltrating FoxP3$^-$ CD4$^+$ T lymphocytes in non-PD-1^{high} expressers. (M–Q) Frequencies of PD-1$^+$ (M), PD-1$^+$TIM-3$^+$ (N), PD-1$^+$TIGIT$^+$ (O), PD-1$^+$CTLA-4$^+$ (P), and PD-1$^+$ICOS$^+$ (Q) cells among FoxP3$^+$CD4$^+$ TILs in non-PD-1^{high} expressers and PD-1^{high} expressers. (R–U) Production of IFN-γ (R), TNF (S), and both IFN-γ and TNF (T) of CD8$^+$ TILs from non-PD-1^{high} expressers and PD-1^{high} expressers on stimulation with anti-CD3 and anti-CD28, and a representative flow cytometry plot (U). *p<0.05; **p<0.01; ***p<0.001; ****p<0.0001. CTLA-4, cytotoxic T-lymphocyte-associated protein-4; FoxP3, forkhead box protein P3; FSC-A, forward scatter area; ICOS, inducible T-cell costimulator; IFN-γ, interferon-γ; NSCLC, non-small-cell lung cancer; PD-1, programmed cell death-1; TIGIT, T cell immunoreceptor with Ig and ITIM domains; TILs, tumor-infiltrating lymphocytes; TIM-3, T cell immunoglobulin and mucin domain-containing protein 3; TNF, tumor necrosis factor.

Table 1 Baseline characteristics of patients

Variables	PD-1^{high} expresser (n=25)	Non-PD-1^{high} expresser (n=71)	P value
Age			0.128
Median (range)	67 (44–86)	64 (35–79)	
Sex			0.004
Male	21 (84.0%)	36 (50.7%)	
Female	4 (16.0%)	35 (49.3%)	
Smoking status			0.001
Current	4 (16.0%)	13 (18.3%)	
Former	15 (60.0%)	14 (19.7%)	
Never	6 (24.0%)	44 (62.0%)	
Stage			0.484
I	11 (44.0%)	35 (49.3%)	
II	7 (28.0%)	24 (33.8%)	
III	7 (28.0%)	11 (16.9%)	
Pathology			<0.001
Adenocarcinoma	13 (52.0%)	64 (90.1%)	
Squamous cell carcinoma	12 (48.0%)	7 (9.9%)	
EGFR or *ALK* alterations			0.026
EGFR mutation	5 (20.0%)	34 (47.9%)	
ALK rearrangement	0 (0.0%)	2 (2.8%)	
Wild type	20 (80.0%)	35 (49.3%)	
PD-L1 expression (TPS)			<0.001
0%	1 (4.0%)	47 (66.2%)	
1%–49%	12 (48.0%)	17 (23.9%)	
≥50%	12 (48.0%)	7 (9.9%)	

ALK, anaplastic lymphoma kinase; EGFR, epidermal growth factor receptor; PD-1, programmed cell death protein 1; PD-L1, programmed death ligand-1; TPS, tumor proportion score.

of 1% and 50%, respectively) and tumor proportion score (figure 3E–G), although prediction of PD-1^{high} expressers based on PD-L1 expression was incomplete (online supplemental figure 10). Moreover, PD-1^{high} expressers had a poorer prognosis than non-PD-1^{high} expressers with respect to disease-free survival after surgical resection (figure 3H). In addition, univariate and multivariate analyses after adjustment for alteration in *EGFR* or *ALK* and PD-L1 positivity confirmed that the presence of distinct PD-1^{high} CD8^{+} TILs independently predicts poor survival outcomes (online supplemental table 2). When subgroup analysis was performed according to the presence or absence of alterations in *EGFR* or *ALK*, this significant association was maintained (figure 3I and J). Intriguingly, the effector cytokine-producing capacity was lower in patients with a smoking history and in tumors with squamous differentiation and/or without alterations in either *EGFR* of *ALK* (online supplemental figure 11). Furthermore, diminished functionality of CD8^{+} TILs was associated with worse disease-free survival (online supplemental figure 11). Taken together, these results indicate that classification based on the PD-1 expression of CD8^{+} TILs facilitates the identification of a patient subgroup associated with a worse prognosis. In addition, this subgroup of patients likely exhibits the clinicopathological characteristics (eg, high PD-L1 expression, *EGFR* and *ALK* wild-type, and previous history of smoking) known to be associated with the benefits from anti-PD-1-based immunotherapy.[20 25 35 36]

Functionality of CD8^{+} TILs from NSCLC patients is further restored after combined immune checkpoint blockade with anti-PD-1 and anti-CTLA-4 antibodies

Since most CD8^{+} TILs from PD-1^{high} expressers were more likely to express multiple immune checkpoints, we examined whether a PD-1 inhibitor in conjunction with a CTLA-4 inhibitor cooperatively restores the function of CD8^{+} TILs. First, we tested whether the functions of CD8^{+} TILs are enhanced by ex vivo single blockade of PD-1 or CTLA-4. Hence, we evaluated the production of IFN-γ and TNF by CD8^{+} TILs on anti-CD3 and anti-CD28 stimulation in the presence or absence of anti-PD-1

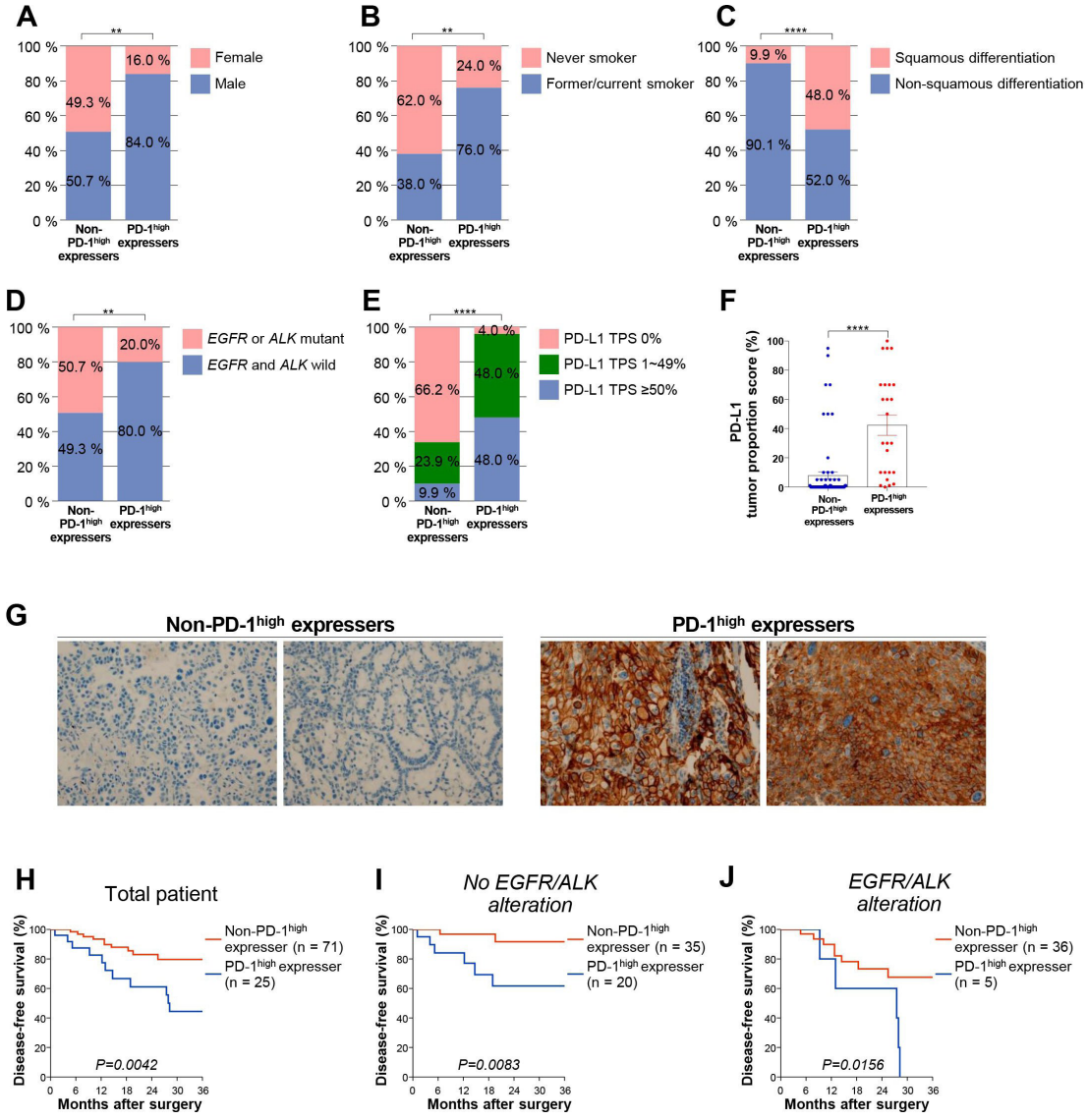

Figure 3 Clinicopathological variables and survival outcomes in non-PD-1^{high} expressers and PD-1^{high} expressers. (A) Distribution of sex, (B) smoking status, (C) histology, (D) presence of oncogenic *EGFR* or *ALK* mutation, and (E) PD-L1 positivity (≥1% and ≥50% as a tumor proportion score) in non-PD-1^{high} expressers and PD-1^{high} expressers. (F) PD-L1 expression as a tumor proportion score in non-PD-1^{high} expressers and PD-1^{high} expressers. (G) Representative immunohistochemistry images of PD-L1 from two non-PD-1^{high} expressers and PD-1^{high} expressers, respectively. (H–J) Disease-free survival of non-PD-1^{high} expressers and PD-1^{high} expressers for all patients (H; n=96), patients with wild-type *EGFR* and *ALK* (I; n=55), and patients with mutant-type *EGFR* or *ALK* (J; n=41). **p<0.01; ****p<0.0001. ALK, anaplastic lymphoma kinase; EGFR, epidermal growth factor receptor; PD-1, programmed cell death-1; PD-L1, programmed death ligand-1; TPS, Tumor Proportion Score.

or anti-CTLA-4 antibodies (figure 4A,B). This functional analysis showed that PD-1 blockade alone increased the capacity of CD8$^+$ TILs to produce IFN-γ, whereas CTLA-4 blockade alone was not as effective. More importantly, the combined PD-1 and CTLA-4 blockade significantly enhanced the polyfunctionality of CD8$^+$ TILs to produce IFN-γ and TNF concurrently on anti-CD3/28 stimulation compared with PD-1 or CTLA-4 blockade alone, suggesting a potential synergism of this combination as witnessed in the CheckMate-227 study.[13] This synergism was more evident in PD-1^{high} expressers than in non-PD-1^{high} expressers (online supplemental figure 12). Collectively, these results indicate that the combined blockade of immune checkpoint inhibitory receptors further restores the polyfunctionality of CD8$^+$ TILs compared with monotherapy, consistent with previous studies.[37 38]

Frequency of PD-1^{high} CD8$^+$ T lymphocytes in peripheral blood predicts two subgroups of NSCLC patients

We next focused on PD-1^{high} CD8$^+$ T lymphocytes in the peripheral blood to examine whether the frequency of these cells can help identify subgroups of NSCLC patients. A significant correlation was found in the plot of the frequency of PD-1^{high} CD8$^+$ T lymphocytes from the peripheral blood and tumor (figure 5A). Notably, the frequency of PD-1$^+$CD8$^+$ T lymphocytes from the peripheral blood was significantly higher in PD-1^{high} expressers than in non-PD-1^{high} expressers (figure 5B). Moreover,

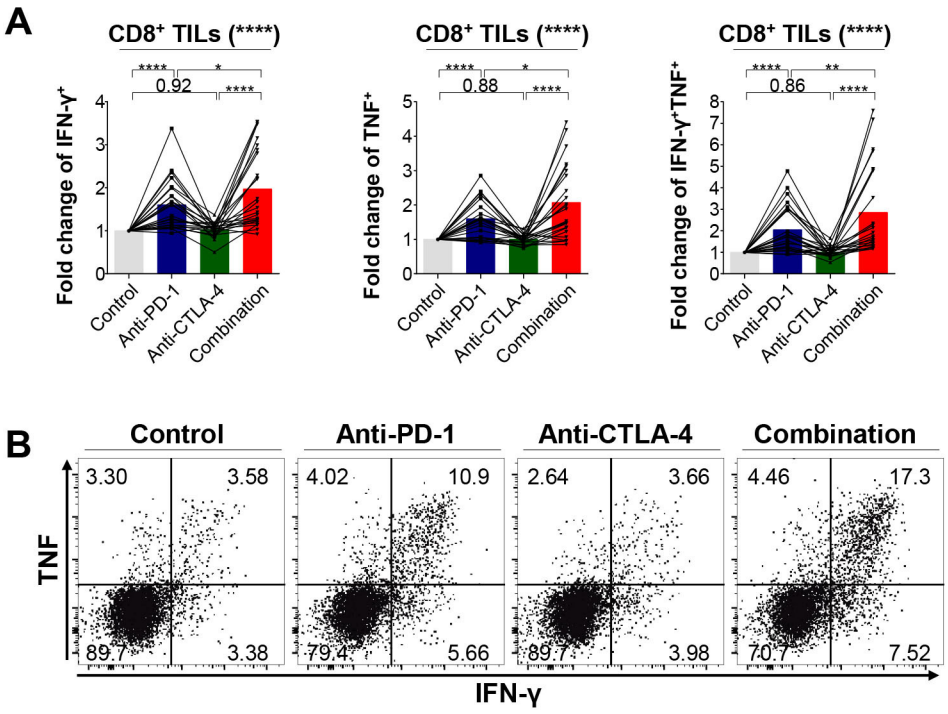

Figure 4 Efficacy of single PD-1 blockade and combined blockade of PD-1 and CTLA-4 on the effector cytokine production of CD8$^+$ TILs (n=24). (A–B) Fold change of IFN-γ$^+$, TNF$^+$, and IFN-γ$^+$TNF$^+$ cells among CD8$^+$ TILs relative to isotype controls on stimulation (A) and representative flow cytometry plot (B). *p<0.05; **p<0.01; ****p<0.0001. CTLA-4, cytotoxic T-lymphocyte-associated protein-4; IFN-γ, interferon-γ; PD-1, programmed cell death-1; TILs, tumor-infiltrating lymphocytes; TNF, tumor necrosis factor.

the frequency of circulating PD-1^{high} CD8$^+$ T lymphocytes predicted PD-1^{high} expressers and non-PD-1^{high} expressers fairly well (figure 5C). Similar findings were obtained in the analysis of tumor-infiltrating FoxP3$^+$ Treg CD4$^+$ T lymphocytes but these effects were not recapitulated in the case of tumor-infiltrating FoxP3$^-$ non-Treg CD4$^+$ lymphocytes (figure 5D–I). Overall, these results further support the potential usefulness of analyzing PD-1^{high} populations from peripheral blood-derived T lymphocytes in the absence of tumor tissues.

DISCUSSION

Reinvigoration of tumor-specific T cells with PD-1 blockade has been established as a standard armamentarium for advanced NSCLC.[39] However, previous studies did not address the distinct exhaustion features of TILs in the context of clinicopathological variables,[33 40] largely limiting the clinical usefulness of these studies. Here, we describe the properties of TILs with differential PD-1 expression in NSCLC that correlated with the distinct features of T-cell exhaustion and activation. Furthermore, we showed that NSCLC patients exhibited profound differences in terms of T-cell exhaustion, indicating that a different response to PD-1 blockade relies on the discrete exhaustion features of TILs at an individual patient level. Finally, we demonstrated that the simultaneous targeting of immune checkpoint inhibitory receptors significantly restores T-cell functionality, assigning translational relevance to current clinical trials and treatment strategies.

The persistent antigenic stimulation witnessed in chronic viral infections and cancer ultimately causes eccentric types of T-cell dysfunction, collectively referred to as T-cell exhaustion.[1–3] During the process of T-cell exhaustion, T cells undergo unique cellular and molecular processes, displaying loss of effector functions, metabolic inertia, diminished self-renewal capacity with loss of stemness, and epigenetic and transcriptional reprogramming. Upregulation of immune checkpoint inhibitory receptors such as PD-1 and CTLA-4 evidently occurs in T-cell exhaustion,[9] highlighting the therapeutic potential of the pharmacological inhibition of these receptors as new strategies for redirecting exhausted T cells to combat cancers. However, an immune checkpoint blockade does not elicit a treatment response in the majority of patients,[17] largely limiting its therapeutic efficacy. Notably, an intricate understanding of T-cell exhaustion using clinical samples is warranted for appropriate patient selection, with suggestions of relevant predictive biomarkers and for enhancing therapeutic efficacy through combination strategies.

Previously, Thommen *et al* identified PD-1 as a marker for defining transcriptionally and functionally distinct CD8$^+$ TILs with predictive implications.[33] Here, we subdivided CD8$^+$ TILs into the PD-1^{neg}, PD-1^{int}, and PD-1^{high} populations based on PD-1 expression. PD-1^{high} CD8$^+$

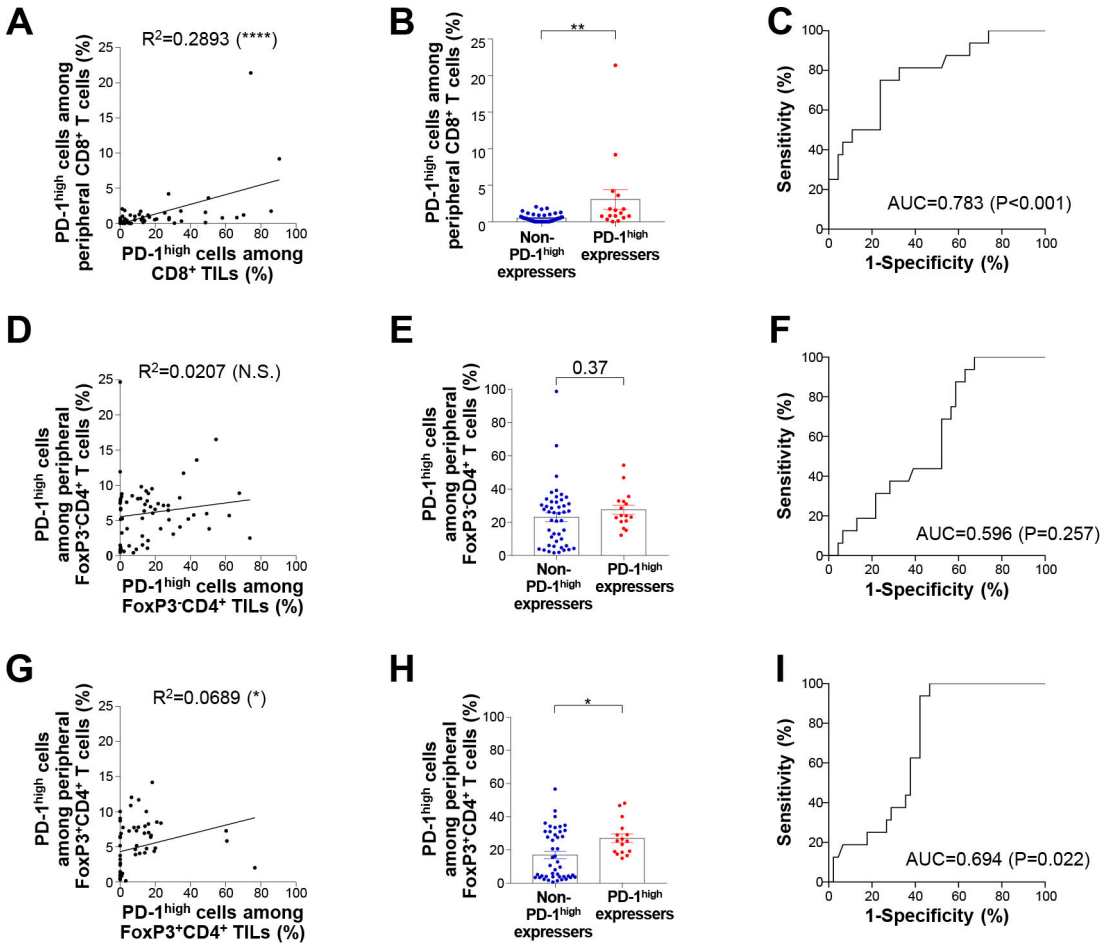

Figure 5 Two subgroups of NSCLC patients can be distinguished by the frequency of peripheral PD-1$^+$ T lymphocytes. (A) Correlation between PD-1^{high} cells among CD8$^+$ TILs and PD-1^{high} cells among peripheral CD8$^+$ T lymphocytes. (B) Frequency of PD-1^{high} cells among peripheral CD8$^+$ T lymphocytes in non-PD-1^{high} expressers and PD-1^{high} expressers. (C) Receiver operative curves describing the performance of the frequency of peripheral PD-1^{high} CD8$^+$ T lymphocytes in distinguishing non-PD-1^{high} expressers and PD-1^{high} expressers. (D) Correlation between PD-1^{high} cells among tumor-infiltrating FoxP3$^-$CD4$^+$ T lymphocytes and PD-1^{high} cells among peripheral FoxP3$^-$CD4$^+$ T lymphocytes. (E) Frequency of PD-1^{high} cells among peripheral FoxP3$^-$CD4$^+$ T lymphocytes in non-PD-1^{high} expressers and PD-1^{high} expressers. (F) Receiver operating characteristic curves describing the performance of the frequency of peripheral PD-1^{high} FoxP3$^-$CD4$^+$ T lymphocytes in distinguishing non-PD-1^{high} expressers and PD-1^{high} expressers. (G) Correlation between PD-1^{high} cells among tumor-infiltrating FoxP3$^+$CD4$^+$ T lymphocytes and PD-1^{high} cells among peripheral FoxP3$^+$CD4$^+$ T lymphocytes. (H) Frequency of PD-1^{high} cells among peripheral FoxP3$^+$CD4$^+$ T lymphocytes in non-PD-1^{high} expressers and PD-1^{high} expressers. (I) Receiver operating characteristic curves describing the performance of the frequency of peripheral PD-1^{high} FoxP3$^+$CD4$^+$ T lymphocytes in distinguishing non-PD-1^{high} expressers and D-1^{high} expressers. AUC, area under the curve; FoxP3, forkhead box protein P3; NSCLC, non-small-cell lung cancer; N.S, not significant; PD-1, programmed cell death-1; TILs, tumor-infiltrating lymphocytes. *p<0.05; **p<0.01; ****p<0.0001.

TILs showed prominent expression of exhaustion-related and activation-related markers compared with PD-1^{neg} and PD-1^{int} CD8$^+$ T cells. More importantly, the enrichment pattern of PD-1^{high} CD8$^+$ TILs identified two NSCLC patient subgroups, and was associated with histological subtypes, PD-L1 expression, alterations in *EGFR* and *ALK*, and history of smoking based on larger cohorts with 96 patients, previously not attempted.[33] Furthermore, the ex vivo reinvigoration of CD8$^+$ TILs was successfully achieved by the combination blockade of PD-1 and CTLA-4, confirming the efficacy of the combined immune checkpoint blockade. Lastly, phenotypes of CD8$^+$ T cells from peripheral blood were highly correlated with those from the TME, suggesting the validity of non-invasive biomarker analysis through blood sampling. Collectively, our findings underscore the translational relevance of a detailed characterization of T-cell exhaustion using clinical samples for leveraging immunotherapeutic strategies in a more efficient manner for NSCLC treatment.

Our study highlights several important issues spanning from T-cell exhaustion biology to routine clinical practice. First, exhausted T-cell populations showed the robust upregulation of markers associated with T-cell activation, indicating that T-cell exhaustion inevitably occurs in the context of T-cell activation. As demonstrated in a previous study, these PD-1^{high} CD8$^+$ T cells are predicted to be reactive to clonal neoantigens commonly shared by tumor cells, which has therapeutic relevance.[41] Moreover,

PD-1^{high} TILs from NSCLC patients share key characteristics with exhausted T cells described in previous studies,[33 34] such as coexpression of multiple immune checkpoint inhibitory receptors as well as tissue-resident markers; they also clearly express higher levels of ICOS and Ki-67 compared with PD-1^{int} or PD-1^{neg} TILs. A striking aspect of this phenomenon is that costimulatory signals can be reinforced for further functional restoration of exhausted T cells. The largely restricted tumor reactivity of PD-1^{high} TILs suggested by recent studies also supports the clinical utility of the simultaneous targeting of coinhibitory and costimulatory receptors.[33]

Second, enrichment of PD-1^{high} CD8^{+} TIL was associated with worse clinical outcomes, thus revealing that the T-cell exhaustion status can be used for the incorporation of immune checkpoint blockade in adjuvant treatment strategies. Guo *et al* already identified that the balance between pre-exhausted T cell subset (CD8-C4-GZMK and CD8-C5-ZNF683 clusters with lower expression of immune checkpoint receptors) and exhausted T cell subset (CD8-C6-LAYN cluster with higher expression of immune checkpoint receptors) was associated with prognosis,[40] consistent with our findings regarding PD-1 expression on CD8^{+} TILs implicated in phenotypic and functional characteristics as well as prognosis. Currently, several studies are investigating whether adjuvant immune checkpoint blockade therapy can lower the incidence of disease relapse and improve survival (NCT02504372, NCT02595944, NCT02486718, and NCT02273375). These studies largely depend on pathological staging for patient enrollment, extrapolating previous strategies for adjuvant chemotherapy. However, our analyses reveal that the extent of T-cell exhaustion was not apparently correlated with disease stage. As in the case of the adjuvant trials focusing on molecular alterations such as *EGFR* mutations,[42] we propose that defining the T-cell exhaustion status can be useful in the enrichment of patients who may derive clinical benefits from immune checkpoint blockade in adjuvant settings. To support this hypothesis, the frequency of PD-1^{high} expressers in our study cohort is similar to the response rate for PD-1 blockade in the prospective studies.[10 14 15] Although there are conflicting data as to whether *EGFR* and *ALK* wild-type tumor are associated with a worse prognosis after surgical resection and an improved response to checkpoint inhibitors,[43–48] our study suggests that the T-cell exhaustion status can be utilized to select patient populations that would be expected to most highly benefit from adjuvant treatment with immune checkpoint inhibitors.

Third, clinicopathological variables traditionally known to be associated with the benefits of PD-1 blockade largely predicted the presence of distinct PD-1^{high} populations in CD8^{+} TILs, although some degree of discordance is evident. For example, PD-L1 expression was higher in PD-1^{high} expressers. In addition, PD-1^{high} expressers were negatively enriched in *EGFR* or *ALK*-altered NSCLC, which is known to have a lower tumor mutation burden with corresponding lower neoantigen levels,[49 50] decreased infiltration of CD8^{+} T cells,[26] and a reduced IFN-γ signature.[49 51] Smokers were also frequently observed among PD-1^{high} expressers (figure 3B), consistent with a previous study demonstrating associations among smoking, chronic obstructive pulmonary disease, and the response to anti-PD-L1/PD-1 inhibitors.[52] This finding is largely consistent with previous studies revealing the plausible association between PD-L1 expression, tumor mutation burden, smoking history, oncogenic driver mutations, and response to PD-1 blockade.[20 25 26] However, lower PD-L1 expression, as well as the presence of *EGFR* mutations and *ALK* rearrangements, do not exclude the possibility of the clinical benefit of PD-1 blockade, reflecting that the crosstalk between tumor-intrinsic molecular alterations and T-cell exhaustion comprehensively dictates the response to PD-1 blockade. Opposing roles of IFN on tumor cells and immune cells can be an example to finely determine anti-PD-1 response.[53] Further comprehensive explorations to define multiple factors to dictate response for PD-1 blockade is required in future studies with a larger sample size.

Fourth, our ex vivo analysis of TILs confirmed that the combined blockade of PD-1 and CTLA-4 cooperatively enhanced effector cytokine production, providing direct evidence for the enhanced efficacy of dual checkpoint inhibitors. In line with this, the CheckMate-227 (NCT02477826) and CheckMate-9LA (NCT03215706) studies have shown robust antitumor activity following the combined use of PD-1 and CTLA-4 inhibitors, which ultimately translated into improved overall survival. Based on these results, the US Food and Drug Administration has approved pembrolizumab plus ipilimumab and nivolumab plus ipilimumab with chemotherapy for the first-line treatment of NSCLC patients. Future investigations of the combined blockade of the PD-1/PD-L1 axis and other immune checkpoint coinhibitory receptors such as TIGIT (NCT03563716) would be clinically relevant. Furthermore, investigating whether inhibition of IFN signaling pathway provoked by checkpoint inhibitors in a tumor-specific manner would bring further benefit for patients treated immunotherapy would be another intriguing area of future research, based on the study conducted by Benci *et al*.[53]

Lastly, non-invasive blood-based biomarker analysis can be used to monitor the T-cell exhaustion status in the TME. Our study showed a noteworthy correlation between the frequency of the PD-1^{high} population in CD8^{+} T cells from the peripheral blood and tumors. Notably, Huang *et al*[54] demonstrated clonal overlap between CD8^{+} T cells from the tumor and peripheral blood, providing evidence that peripheral CD8^{+} T cells can be used as a non-invasive marker for the suspected characteristics of CD8^{+} TILs. Indeed, several studies have proposed using PD-1^{+}CD8^{+} T cells or their characteristics as predictors of the response to checkpoint inhibitors.[54–56] The analysis of the currently suggested biomarkers for PD-1 blockade, such as PD-L1 expression, tumor mutation burden, pre-existing T cell

infiltration, and transcription signatures, necessitates the collection of tissue specimens, which is apparently associated with a higher risk of procedure-related comorbidity and mortality, especially in NSCLC patients.[27 57] Considering these aspects, blood-based biomarker analysis can be a valuable tool for serial immune monitoring. We anticipate that our findings can be validated by matching tumor samples with blood samples in future clinical trials.

In conclusion, we showed a distinct exhaustion status of TILs in patients with NSCLC at both the intraindividual and interindividual levels. Our results indicate that the characteristics of T cell exhaustion measured using clinical samples have therapeutic implications in terms of understanding T-cell exhaustion biology, deducing relevant biomarkers, and designing future clinical trials, providing compelling evidence for the fact that the exhaustion features of TILs determine the response to PD-1 blockade. Future studies should examine whether the selective targeting of PD-1^{high} populations can further enhance the clinical benefits of immunotherapy in view of the distinguished cellular states of these cells, and whether PD-1 blockade can systemically influence the T-cell fate with regard to their exhaustion in the TME.

Author affiliations
[1]Division of Medical Oncology, Department of Internal Medicine, Yonsei Cancer Center, Yonsei University College of Medicine, Seoul, Republic of Korea
[2]Department of Radiation Oncology, Yonsei Cancer Center, Yonsei University College of Medicine, Seoul, Republic of Korea
[3]Department of Biochemistry, College of Life Science and Biotechnology, Yonsei University, Seoul, Republic of Korea
[4]Department of Pathology, Yonsei University College of Medicine, Seoul, Republic of Korea
[5]Department of Thoracic and Cardiovascular Surgery, Yonsei University College of Medicine, Seoul, Republic of Korea

Acknowledgements We thank all patients who participated in this study.

Contributors Responsible for the overall content as guarantor: HRK. Conception and design: SYP, S-JH, and HRK. Financial support: CGK, SYP, S-JH, and HRK. Provision of study materials or patients: HSS, HIY, SYP, S-JH, and HRK. Collection and assembly of data: CGK, GK, KHK, SP, SS, and DY. Data analysis and interpretation: CGK, GK, KHK, SP, SS, HSS, HIY, SYP, S-JH, and HRK. Manuscript writing: CGK, GK, SYP, S-JH, and HRK. All authors read and approved the final manuscript.

Funding This research was supported by the Bio & Medical Technology Development Program of the National Research Foundation funded by the Ministry of Science and ICT (NRF-2019M3A9B6065231, 2017M3A9E802971, and 2017M3A9E9072669 to HRK and 2019M3A9B6065221, 2018R1A2A1A05076997, and 2017R1A5A1014560 to S-JH), Severance Hospital Research fund for Clinical excellence (C-2021-0016 to HRK), and Young Medical Scientist Research Grant Program of the Daewoong Foundation (DY20206P to CGK).

Competing interests None declared.

Patient consent for publication Consent obtained directly from patient(s)

Ethics approval This study was approved by the Yonsei Cancer Center Institutional Review Board (4-2018-1210).

Provenance and peer review Not commissioned; externally peer reviewed.

Data availability statement Data are available on reasonable request. Data are available from the corresponding author HRK on reasonable request.

ORCID iDs
Seong Yong Park http://orcid.org/0000-0002-5180-3853
Sang-Jun Ha http://orcid.org/0000-0002-1192-6031
Hye Ryun Kim http://orcid.org/0000-0002-1842-9070

REFERENCES

1 McLane LM, Abdel-Hakeem MS, Wherry EJ. Cd8 T cell exhaustion during chronic viral infection and cancer. *Annu Rev Immunol* 2019;37:457–95.
2 Blank CU, Haining WN, Held W, *et al*. Defining 'T cell exhaustion'. *Nat Rev Immunol* 2019;19:665–74.
3 Beltra J-C, Manne S, Abdel-Hakeem MS, *et al*. Developmental relationships of four exhausted CD8$^+$ T cell subsets reveals underlying transcriptional and epigenetic landscape control mechanisms. *Immunity* 2020;52:825–41.
4 Kim CG, Jang M, Kim Y, *et al*. VEGF-A drives TOX-dependent T cell exhaustion in anti-PD-1-resistant microsatellite stable colorectal cancers. *Sci Immunol* 2019;4:1. doi:10.1126/sciimmunol.aay0555
5 Alfei F, Kanev K, Hofmann M, *et al*. TOX reinforces the phenotype and longevity of exhausted T cells in chronic viral infection. *Nature* 2019;571:265–9.
6 Scott AC, Dündar F, Zumbo P, *et al*. TOX is a critical regulator of tumour-specific T cell differentiation. *Nature* 2019;571:270–4.
7 Khan O, Giles JR, McDonald S, *et al*. TOX transcriptionally and epigenetically programs CD8$^+$ T cell exhaustion. *Nature* 2019;571:211–8.
8 Wei SC, Duffy CR, Allison JP. Fundamental mechanisms of immune checkpoint blockade therapy. *Cancer Discov* 2018;8:1069–86.
9 Ribas A, Wolchok JD. Cancer immunotherapy using checkpoint blockade. *Science* 2018;359:1350–5.
10 Garon EB, Rizvi NA, Hui R, *et al*. Pembrolizumab for the treatment of non-small-cell lung cancer. *N Engl J Med* 2015;372:2018–28.
11 Reck M, Rodríguez-Abreu D, Robinson AG, *et al*. Pembrolizumab versus chemotherapy for PD-L1-positive non-small-cell lung cancer. *N Engl J Med* 2016;375:1823–33.
12 Paz-Ares L, Luft A, Vicente D, *et al*. Pembrolizumab plus chemotherapy for squamous non-small-cell lung cancer. *N Engl J Med* 2018;379:2040–51.
13 Hellmann MD, Paz-Ares L, Bernabe Caro R, *et al*. Nivolumab plus ipilimumab in advanced non-small-cell lung cancer. *N Engl J Med* 2019;381:2020–31.
14 Brahmer J, Reckamp KL, Baas P, *et al*. Nivolumab versus docetaxel in advanced squamous-cell non-small-cell lung cancer. *N Engl J Med* 2015;373:123–35.
15 Borghaei H, Paz-Ares L, Horn L, *et al*. Nivolumab versus docetaxel in advanced Nonsquamous non-small-cell lung cancer. *N Engl J Med* 2015;373:1627–39.
16 Gandhi L, Rodríguez-Abreu D, Gadgeel S, *et al*. Pembrolizumab plus chemotherapy in metastatic non-small-cell lung cancer. *N Engl J Med* 2018;378:2078–92.
17 Mayes PA, Hance KW, Hoos A. The promise and challenges of immune agonist antibody development in cancer. *Nat Rev Drug Discov* 2018;17:509–27.
18 Doroshow DB, Sanmamed MF, Hastings K, *et al*. Immunotherapy in non-small cell lung cancer: facts and hopes. *Clin Cancer Res* 2019;25:4592–602.
19 Yu H, Boyle TA, Zhou C, *et al*. PD-L1 expression in lung cancer. *J Thorac Oncol* 2016;11:964–75.
20 Rizvi H, Sanchez-Vega F, La K, *et al*. Molecular determinants of response to anti-programmed cell death (PD)-1 and anti-programmed death-ligand 1 (PD-L1) blockade in patients with non-small-cell lung cancer profiled with targeted next-generation sequencing. *J Clin Oncol* 2018;36:633–41.

21 Sun R, Limkin EJ, Vakalopoulou M, *et al*. A radiomics approach to assess tumour-infiltrating CD8 cells and response to anti-PD-1 or anti-PD-L1 immunotherapy: an imaging biomarker, retrospective multicohort study. *Lancet Oncol* 2018;19:1180–91.
22 Rizvi NA, Hellmann MD, Snyder A, *et al*. Cancer immunology. mutational landscape determines sensitivity to PD-1 blockade in non-small cell lung cancer. *Science* 2015;348:124–8.
23 Hugo W, Zaretsky JM, Sun L, *et al*. Genomic and transcriptomic features of response to anti-PD-1 therapy in metastatic melanoma. *Cell* 2016;165:35–44.
24 Chowell D, Morris LGT, Grigg CM, *et al*. Patient HLA class I genotype influences cancer response to checkpoint blockade immunotherapy. *Science* 2018;359:582–7.
25 Sacher AG, Gandhi L. Biomarkers for the clinical use of PD-1/PD-L1 inhibitors in non-small-cell lung cancer: a review. *JAMA Oncol* 2016;2:1217–22.
26 Gainor JF, Shaw AT, Sequist LV, *et al*. EGFR mutations and ALK rearrangements are associated with low response rates to PD-1 pathway blockade in non-small cell lung cancer: a retrospective analysis. *Clin Cancer Res* 2016;22:4585–93.
27 Kim CG, Hong MH, Kim KH, *et al*. Dynamic changes in circulating PD-1^{+}CD8^{+} T lymphocytes for predicting treatment response to PD-1 blockade in patients with non-small-cell lung cancer. *Eur J Cancer* 2021;143:113–26.
28 Jakubek Y, Lang W, Vattathil S, *et al*. Genomic landscape established by allelic imbalance in the cancerization field of a normal appearing airway. *Cancer Res* 2016;76:3676–83.
29 Speiser DE, Ho P-C, Verdeil G. Regulatory circuits of T cell function in cancer. *Nat Rev Immunol* 2016;16:599–611.
30 Duhen T, Duhen R, Montler R, *et al*. Co-expression of CD39 and CD103 identifies tumor-reactive CD8 T cells in human solid tumors. *Nat Commun* 2018;9:2724.
31 O'Brien SM, Klampatsa A, Thompson JC, *et al*. Function of human tumor-infiltrating lymphocytes in early-stage non-small cell lung cancer. *Cancer Immunol Res* 2019;7:896–909.
32 Bally APR, Austin JW, Boss JM. Genetic and epigenetic regulation of PD-1 expression. *J Immunol* 2016;196:2431–7.
33 Thommen DS, Koelzer VH, Herzig P, *et al*. A transcriptionally and functionally distinct PD-1^{+} CD8^{+} T cell pool with predictive potential in non-small-cell lung cancer treated with PD-1 blockade. *Nat Med* 2018;24:994–1004.
34 Thommen DS, Schreiner J, Müller P, *et al*. Progression of lung cancer is associated with increased dysfunction of T cells defined by coexpression of multiple inhibitory receptors. *Cancer Immunol Res* 2015;3:1344–55.
35 Mazieres J, Drilon A, Lusque A, *et al*. Immune checkpoint inhibitors for patients with advanced lung cancer and oncogenic driver alterations: results from the IMMUNOTARGET registry. *Ann Oncol* 2019;30:1321–8.
36 Gettinger SN, Horn L, Gandhi L, *et al*. Overall survival and long-term safety of nivolumab (anti-programmed death 1 antibody, BMS-936558, ONO-4538) in patients with previously treated advanced non-small-cell lung cancer. *J Clin Oncol* 2015;33:2004–12.
37 Curran MA, Montalvo W, Yagita H, *et al*. PD-1 and CTLA-4 combination blockade expands infiltrating T cells and reduces regulatory T and myeloid cells within B16 melanoma tumors. *Proc Natl Acad Sci U S A* 2010;107:4275–80.
38 Wei SC, Anang N-AAS, Sharma R, *et al*. Combination anti-CTLA-4 plus anti-PD-1 checkpoint blockade utilizes cellular mechanisms partially distinct from monotherapies. *Proc Natl Acad Sci U S A* 2019;116:22699–709.
39 Esencay M, Watson A, Mukherjee K, *et al*. Biomarker strategy in lung cancer. *Nat Rev Drug Discov* 2018;17:13–14.
40 Guo X, Zhang Y, Zheng L, *et al*. Global characterization of T cells in non-small-cell lung cancer by single-cell sequencing. *Nat Med* 2018;24:978–85.
41 McGranahan N, Furness AJS, Rosenthal R, *et al*. Clonal neoantigens elicit T cell immunoreactivity and sensitivity to immune checkpoint blockade. *Science* 2016;351:1463–9.
42 Wu Y-L, Tsuboi M, He J, *et al*. Osimertinib in resected EGFR-mutated non-small-cell lung cancer. *N Engl J Med* 2020;383:1711–23.
43 Kim YT, Seong YW, Jung YJ, *et al*. The presence of mutations in epidermal growth factor receptor gene is not a prognostic factor for long-term outcome after surgical resection of non-small-cell lung cancer. *J Thorac Oncol* 2013;8:171–8.
44 Kosaka T, Yatabe Y, Onozato R, *et al*. Prognostic implication of EGFR, KRAS, and TP53 gene mutations in a large cohort of Japanese patients with surgically treated lung adenocarcinoma. *J Thorac Oncol* 2009;4:22–9.
45 Park IK, Hyun K, Kim ER, *et al*. The prognostic effect of the epidermal growth factor receptor gene mutation on recurrence dynamics of lung adenocarcinoma. *Eur J Cardiothorac Surg* 2018;54:1022–7.
46 Matsuura Y, Ninomiya H, Ichinose J, *et al*. Prognostic impact and distinctive characteristics of surgically resected anaplastic lymphoma kinase-rearranged lung adenocarcinoma. *J Thorac Cardiovasc Surg* 2020. doi:10.1016/j.jtcvs.2020.09.120. [Epub ahead of print: 08 Oct 2020].
47 Tao H, Shi L, Zhou A, *et al*. Distribution of EML4-ALK fusion variants and clinical outcomes in patients with resected non-small cell lung cancer. *Lung Cancer* 2020;149:154–61.
48 Blackhall FH, Peters S, Bubendorf L, *et al*. Prevalence and clinical outcomes for patients with ALK-positive resected stage I to III adenocarcinoma: results from the European thoracic oncology platform Lungscape project. *J Clin Oncol* 2014;32:2780–7.
49 Qiao M, Jiang T, Liu X, *et al*. Immune checkpoint inhibitors in EGFR-mutated NSCLC: dusk or dawn? *J Thorac Oncol* 2021;16:1267–88.
50 Schrock AB, Li SD, Frampton GM, *et al*. Pulmonary sarcomatoid carcinomas commonly harbor either potentially targetable genomic alterations or high tumor mutational burden as observed by comprehensive genomic profiling. *J Thorac Oncol* 2017;12:932–42.
51 Higgs BW, Morehouse CA, Streicher K, *et al*. Interferon gamma messenger RNA signature in tumor biopsies predicts outcomes in patients with non-small cell lung carcinoma or urothelial cancer treated with Durvalumab. *Clin Cancer Res* 2018;24:3857–66.
52 Mark NM, Kargl J, Busch SE, *et al*. Chronic obstructive pulmonary disease alters immune cell composition and immune checkpoint inhibitor efficacy in non-small cell lung cancer. *Am J Respir Crit Care Med* 2018;197:325–36.
53 Benci JL, Johnson LR, Choa R, *et al*. Opposing functions of interferon coordinate adaptive and innate immune responses to cancer immune checkpoint blockade. *Cell* 2019;178:933–48.
54 Huang AC, Postow MA, Orlowski RJ, *et al*. T-cell invigoration to tumour burden ratio associated with anti-PD-1 response. *Nature* 2017;545:60–5.
55 Kim KH, Cho J, Ku BM. Correction: the first-week proliferative response of peripheral blood PD-1^{+}CD8+ T cells predicts the response to anti-PD-1 therapy in solid tumors. *Clin Cancer Res* 2020;26:6610.
56 Kamphorst AO, Pillai RN, Yang S, *et al*. Proliferation of PD-1+ CD8 T cells in peripheral blood after PD-1-targeted therapy in lung cancer patients. *Proc Natl Acad Sci U S A* 2017;114:4993–8.
57 Kim CG, Kim KH, Pyo K-H, *et al*. Hyperprogressive disease during PD-1/PD-L1 blockade in patients with non-small-cell lung cancer. *Ann Oncol* 2019;30:1104–13.

Supplementary Table 1. Lists of antibodies

Antigen	Manufacturer	Catalog number
CD3	Biolegend	317329
CD4	Biolegend	300556
CD4	BD Biosciences	560837
CD8	Biolegend	301040
CD8	BD Biosciences	565165
CD25	BD Biosciences	561405
CD28	Biolegend	302945
CD39	Biolegend	328210
CD45	BD Biosciences	560178
CD103	Biolegend	350230
CD152 (CTLA-4)	Biolegend	369608
CD274 (PD-L1)	BD Biosciences	557924
CD278 (ICOS)	Biolegend	313525
CD279 (PD-1)	Biolegend	329920
CD326 (EpCAM)	BD Biosciences	565685
CD366 (TIM-3)	R&D systems	FAB2365G
FoxP3	Biolegend	320108
IFN-γ	Biolegend	502512
IFN-γ	BD Biosciences	564039
Ki-67	BD Biosciences	561277
Ki-67	Biolegend	350530
TIGIT	R&D systems	FAB7898A
TNF	Biolegend	502930
TNF	BD Biosciences	557647

CD, cluster of differentiation; CTLA-4, cytotoxic T-lymphocyte-associated protein 4; FoxP3, forkhead box P3; ICOS, inducible T-cell COStimulator; IFN, interferon; PD-1, programmed cell death protein 1; TIGIT, T cell immunoreceptor with Ig and ITIM domains; TIM-3, T-cell immunoglobulin and mucin-domain containing-3; TNF, tumor necrosis factor.

Supplementary Table 2. Univariate and multivariate analysis for disease-free survival

Index	Univariate analysis		Multivariate analysis	
	HR (95% CI)	***P* value**	**HR (95% CI)**	***P* value**
Age				
<65 years	Reference	0.796		
≥65 years	1.120 (0.475-2.641)			
Sex				
Female	Reference	0.253		
Male	0.606 (0.257-1.430)			
Smoking status				
Non-smoker	Reference	0.417		
Former/current smoker	0.698 (0.293-1.663)			
Stage				
I, II	Reference	0.107		
III	2.112 (0.851-5.244)			
Histology				
Adenocarcinoma	Reference	0.172		
Squamous cell carcinoma	1.935 (0.750-4.993)			
EGFR or *ALK* alterations				
Absent	Reference	0.071	Reference	0.006
Present	2.254 (0.933-5.443)		3.679 (1.447-9.353)	
PD-L1 expression				
Negative	Reference	0.069	Reference	0.211
Positive	2.413 (0.935-6.227)		2.010 (0.674-5.997)	
PD-1 expression				
Non-PD-1^{high} expresser	Reference	0.007	Reference	0.018
PD-1^{high} expresser	3.275 (1.386-7.737)		3.265 (1.224-8.712)	

ALK, anaplastic lymphoma kinase; CI, confidence interval; *EGFR*, epidermal growth factor receptor; HR, hazard ratio; PD-1, programmed cell death protein 1; PD-L1, programmed death ligand-1.

Figure S1

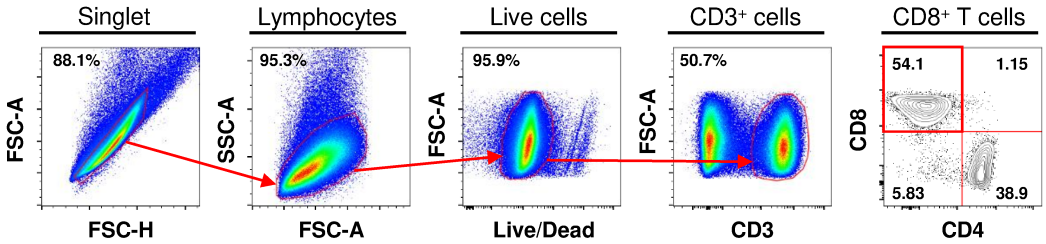

Supplementary Figure 1. Gating strategies for flow cytometry.

Figure S2

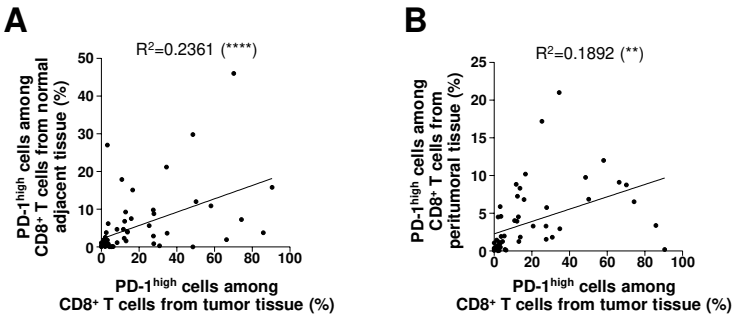

Supplementary Figure 2. Correlation of the frequency of PD-1^{high} T cells from normal adjacent tissues, peritumoral tissues, and tumor tissues. (A) Correlation of the frequencies of PD-1^{high} T cells from normal adjacent tissues and tumor tissues. (B) Correlation of the frequency of PD-1^{high} T cells from peritumoral tissues and tumor tissues.

Figure S3

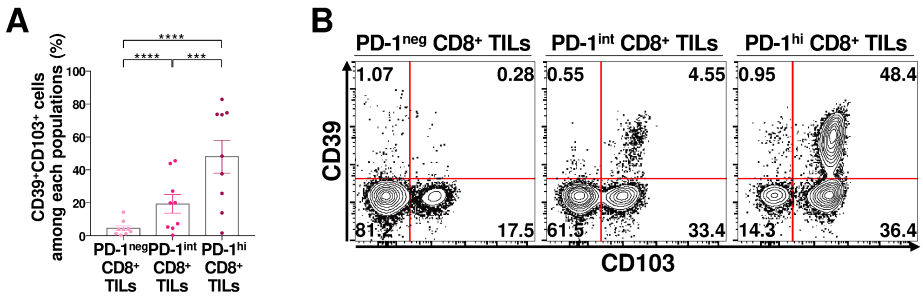

Supplementary Figure 3. Expression of tissue-resident markers in CD8⁺ TILs according to PD-1 level. (A) Frequency of CD39⁺CD103⁺ cells among CD8⁺ TILs (A) and representative flow cytometry plot (B).

Figure S4

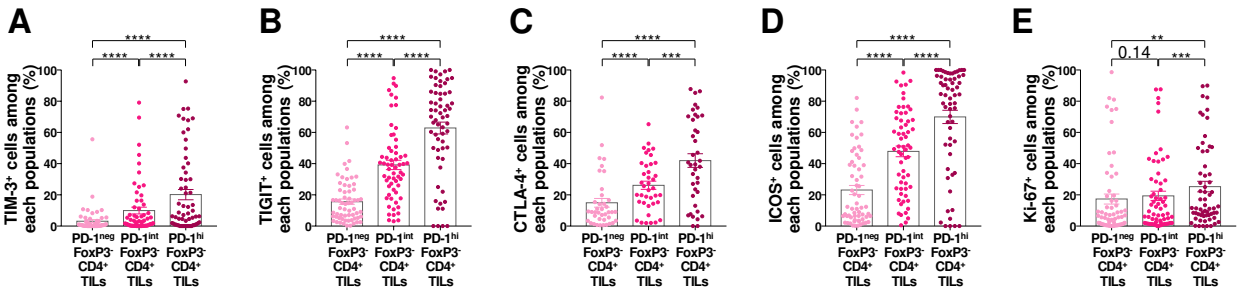

Supplementary Figure 4. Expression of exhaustion- and activation-related molecules on FoxP3⁻CD4⁺ TILs according to PD-1 expression. (A–E) Frequency of TIM-3⁺ (A), TIGIT⁺ (B), CTLA-4⁺ (C), ICOS⁺ (D), and Ki-67⁺ (E) cells among FoxP3⁻CD4⁺ TILs.

Figure S5

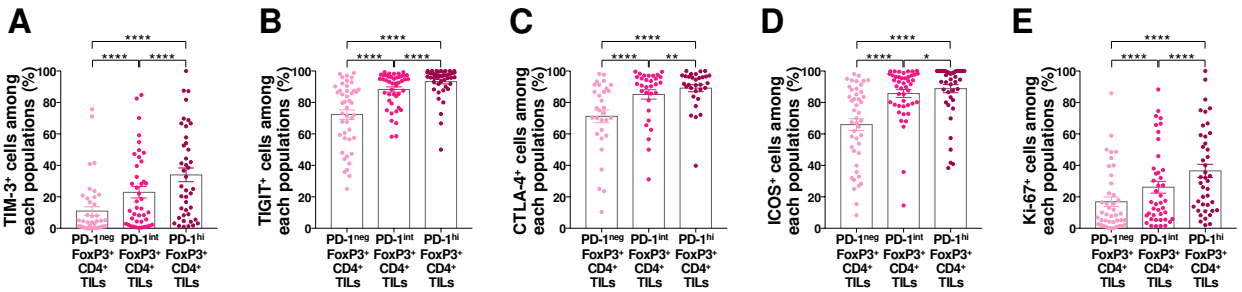

Supplementary Figure 5. Expression of exhaustion- and activation-related molecules on FoxP3⁺CD4⁺ TILs according to PD-1 expression. (A–E) Frequency of TIM-3⁺ (A), TIGIT⁺ (B), CTLA-4⁺ (C), ICOS⁺ (D), and Ki-67⁺ (E) cells among FoxP3⁺CD4⁺ TILs.

Figure S6

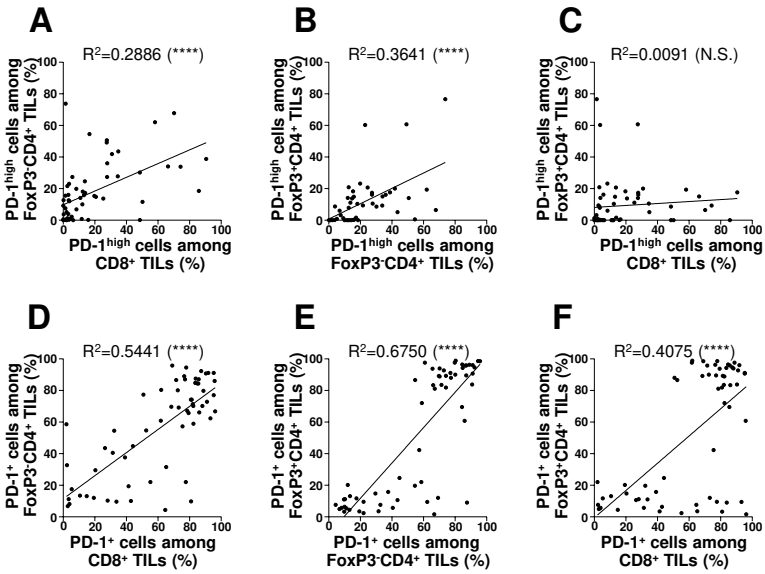

Supplementary Figure 6. Correlation of PD-1 expression between each T cell population. (A-B) Correlations of the frequencies of tumor-infiltrating PD-1^{high} CD8^{+} T lymphocytes, PD-1^{high} FoxP3^{-}CD4^{+} T lymphocytes, PD-1^{high} FoxP3^{+}CD4^{+} T lymphocytes (C-D), PD-1^{+} CD8^{+} T lymphocytes, PD-1^{+} FoxP3^{-}CD4^{+} T lymphocytes, and PD-1^{+} FoxP3^{+}CD4^{+} T lymphocytes (E-F).

Figure S7

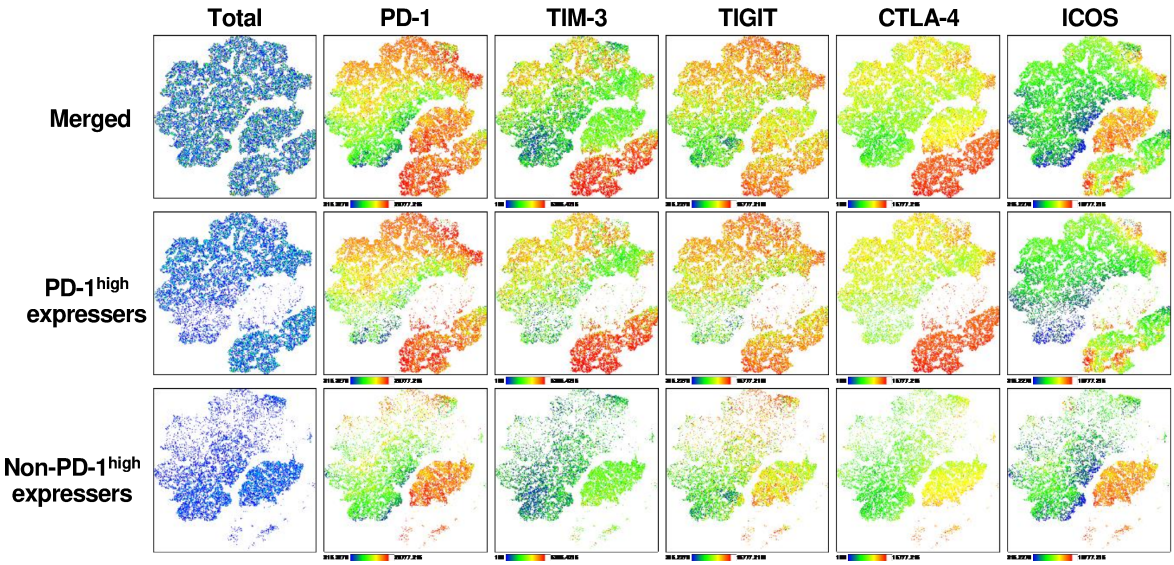

Supplementary Figure 7. t-SNE analysis of the expression of PD-1, TIM-3, TIGIT, CTLA-4, ICOS, and Ki-67 in CD8+ TILs from PD-1high expressers (n = 3) and non-PD-1high expressers (n = 3). t-SNE visualization of flow cytometry data was based on 20,000 randomly selected live and singlet-gated cells isolated from each sample.

Figure S8

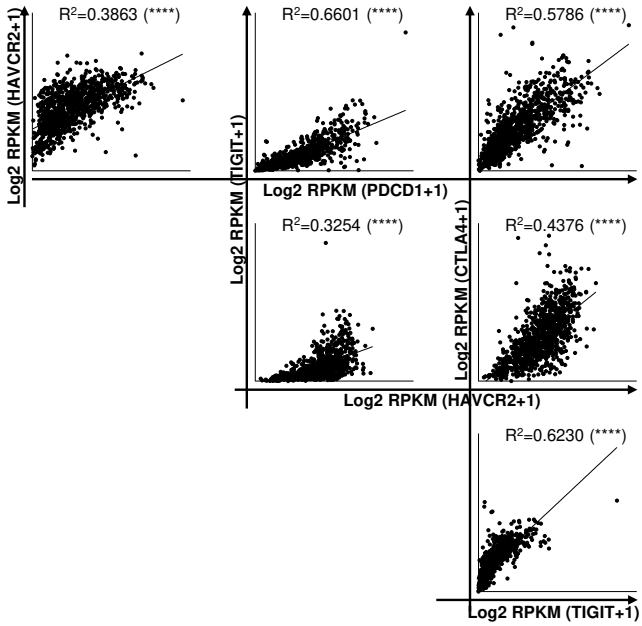

Supplementary Figure 8. Correlations of the expression levels of various immune checkpoint receptors in the TCGA NSCLC cohort.

Figure S9

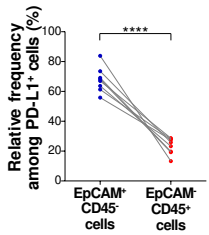

Supplementary Figure 9. Frequency of EpCAM$^+$CD45$^-$ cells and EpCAM$^-$CD45$^+$ cells among PD-L1$^+$ cells from tumor tissue (n = 8).

Figure S10

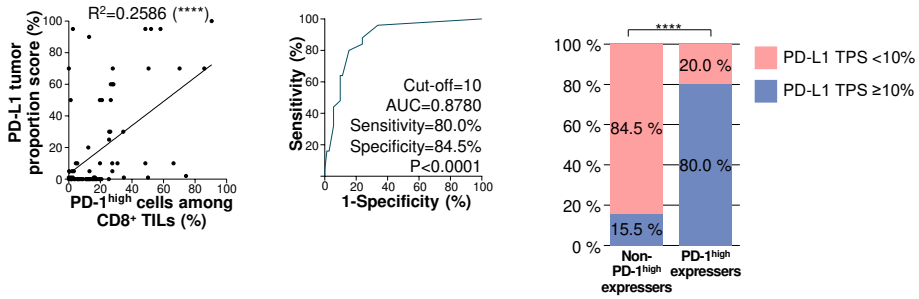

Supplementary Figure 10. Prediction of non-PD-1^{high} expressers and PD-1^{high} expressers based on PD-L1 expression. (A) Correlation between PD-L1 tumor proportion score and PD-1 expression on CD8^{+} TILs. (B) Performance power of PD-L1 tumor proportion score in discriminating non-PD-1^{high} expressers and PD-1^{high} expressers. (C) PD-L1 expression (≥10% as a tumor proportion score) in non-PD-1^{high} expressers and PD-1^{high} expressers.

Figure S11

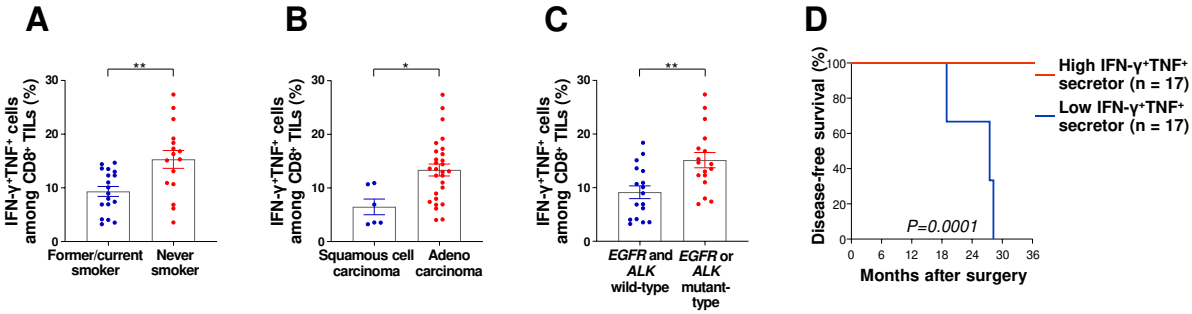

Supplementary Figure 11. Effector cytokine production of CD8⁺ TILs upon stimulation with anti-CD3 and anti-CD28 according to clinicopathologic characteristics and survival outcomes. (A–C) Frequencies of IFN-γ and TNF-producing CD8⁺ TILs according to smoking history (A), histology (B), and *EGFR* or *ALK* alterations (C). (D) Disease-free survival of patients according to IFN-γ and TNF-producing capacity. Patients were categorized based on the median value of the frequency of IFN-γ⁺TNF⁺ CD8⁺ TILs.

Figure S12

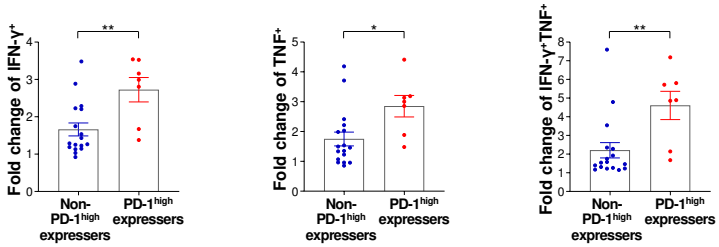

Supplementary Figure 12. Efficacy of combined blockade of PD-1 and CTLA-4 on the effector cytokine production of CD8⁺ TILs (n = 24). Fold change of IFN-γ⁺, TNF⁺, and IFN-γ⁺TNF⁺ cells among CD8⁺ TILs from non-PD-1^{high} expressers (n = 17) and PD-1^{high} expressers (n = 7) relative to isotype controls upon stimulation.